Distribution of geometric quantum discord in photon-added coherent states

M. Daoud[a,b,c1], **W. Kaydi**[d,e 2] and **H. El Hadfi** [d,e 3]

[a] *Max Planck Institute for the Physics of Complex Systems, Dresden, Germany*

[b] *Abdus Salam International Centre for Theoretical Physics, Miramare, Trieste, Italy*

[c] *Department of Physics , Faculty of Sciences, University Ibnou Zohr, Agadir , Morocco*

[d] *LPHE-Modeling and Simulation, Faculty of Sciences, University Mohammed V, Rabat, Morocco*

[e] *Centre of Physics and Mathematics (CPM), University Mohammed V, Rabat, Morocco*

Abstract

We examine the influence of photon excitation on the monogamy property of quantum discord in tripartite coherent states of Greenberger-Horne-Zeilinger type. The Hilbert-Schmidt norm is used as quantifier of pairwise quantum correlations. The geometric quantum discord in all bipartite subsystems are explicitly given. We show that the geometric discord is monogamous for any photon excitation order.

[1]email: m_daoud@hotmail.com
[2]email: kaydi.smp@gmail.com
[3]email: hanane.elhadfi@gmail.com

1 Introduction

Entangled coherent states have found various applications in quantum information science (for a recent review see [1]). In fact, they have been recognized as a valuable resource in quantum teleportation [2, 3, 4, 5, 6, 7], quantum networks [8], quantum logical encoding [9], quantum computation [10], quantum information processing [11] and quantum metrology [12, 13]. Despite their extreme sensitivity to environmental effects, several experimental schemes were proposed for their production [14, 15, 16, 17, 18, 19]. Many protocols for quantum information processing use coherent states as either continuous or discrete variables. In a discrete setting, the information is encoded in superpositions of coherent states [20] like for instance the encoding scheme of logical qubits in even and odd superpositions of Glauber coherent states: $|0\rangle \longrightarrow |\alpha\rangle + |-\alpha\rangle$ and $|1\rangle \longrightarrow |\alpha\rangle - |-\alpha\rangle$ ($\alpha \in \mathbb{C}$). In this picture, balanced superpositions of n-partite Glauber coherent states of type [21]

$$|\psi_n\rangle \backsim |\alpha\rangle_1 \otimes |\alpha\rangle_2 \otimes \cdots \otimes |\alpha\rangle_n \pm |-\alpha\rangle_1 \otimes -|\alpha\rangle_2 \otimes \cdots \otimes |-\alpha\rangle_n$$

provide a physical tool to encode n logical qubits system. This kind of multipartite Glauber states includes the bipartite states ($n = 2$), commonly termed in the literature, quasi-Bell coherent states in analogy with the four Bell states defined for two dimensional quantum systems [22]. For $n = 3$, the states $|\psi_n\rangle$ coincide with quasi-GHZ coherent states [23] which constitute the nonorthogonal analogue of the usual Greenberger-Horne-Zeilinger three qubit states [24]. Entanglement properties of quasi-Bell ($n = 2$) and quasi-GHZ coherent states ($n = 3$) were initially investigated using the formalism of concurrence or equivalently entanglement of formation [21, 22]. Quantum discord, introduced in [25, 26], which goes beyond entanglement of formation, was also considered to evaluate the pairwise quantum discord in multipartite coherent states [27, 28, 29, 30]. The entropy-based quantum discord involves optimization procedure that is, in general, challenging to achieve analytically. To avoid this difficulty and to get computable expressions of bipartite quantum correlations a geometric variant of quantum discord was proposed in [31]. It uses the Hilbert-Schmidt distance as a measure to distinguish between quantum and classical correlations. This geometric quantifier was employed to determine the pairwise correlations in multipartite states of type $|\psi_n\rangle$ [30, 32, 33].

In the other hand, an important issue, in investigating multipartite entangled coherent states, concerns the influence of the environment on the evolution of quantum correlations. In this context, bipartite correlations in single mode excited entangled quasi-Bell [34, 35] and quasi-GHZ coherent states [36] were investigated to analyze the effect of the photon excitations processes. Interesting results were derived in [34, 35, 36] where the pairwise quantum correlations are quantified by means of Wootters concurrence [37]. In this paper, we use the Hilbert-Schmidt distance as quantifier of bipartite quantum correlations to study the distribution of quantum correlation in photon added quasi-GHZ coherent states. Another important aspect is the monogamy property of the geometric discord which limits the free shareability and subsequently imposes severe restrictions on the distribution of quantum correlations between the different parts of the system. The monogamy property can be summarized as follows. Let D_{12} denote the shared geometric quantum discord between the modes 1 and 2. Similarly,

we denote by D_{23} the geometric measure of the quantum correlation between 2 and 3 and $D_{1|23}$ the correlation shared between the mode 1 and the composite subsystem 23 comprising 2 and 3. The geometric quantum discord is monogamous if, and only if, the following inequality

$$D_{1|23} \geq D_{12} + D_{23}$$

is satisfied. In this respect, to establish the conditions under which the geometric quantum discord is monogamous requires the determination of pairwise quantum correlations between the three modes. It worth noticing that the concept of monogamy of quantum correlations was first discussed by Coffman, Kundo and Wootters in 2001 [38] for the entanglement of formation in three qubits. It was generalized after to multi-qubit systems [39] as well as other measures like quantum discord and its geometric variant [40, 41, 42, 43, 44, 45].

The paper is organized as follows. In section 2, we introduce photon added coherent states of Greenberger-Horne-Zeilinger type. In particular we discuss the different bi-partitions of this class of tripartite states. For each bipartite subsystem a suitable qubit mapping is defined. The pairwise quantum correlations, quantified by Hilbert-Schmidt distance, in quasi-GHZ coherent states are derived in section 3. The influence of the photon addition processes is discussed. A special attention is devoted to the limiting case corresponding to photon added states of W-type ($|\alpha| \longrightarrow \infty$). The monogamy relation of geometric discord is examined in section 3. A special emphasis is devoted to the evolution of the geometric quantum discord deficit versus photon excitations number. Concluding remarks close this paper.

2 Photon added coherent states of GHZ type and qubit encoding

2.1 Excitations of quasi-GHZ coherent states

An interesting class of nonclassical states in quantum optics consists of the photon-added coherent states [46]. They result through successive applications of the creation operator a^+ on the Glauber coherent state

$$|\alpha\rangle = e^{-\frac{|\alpha|^2}{2}} \sum_{n=0}^{\infty} \frac{\alpha^n}{\sqrt{n!}} |n\rangle. \tag{1}$$

Denoting by m the number of added quanta, the explicit form of a normalized m-photon added coherent state in the Fock states basis $\{|n\rangle,\ n \in \mathbb{N}\}$ is

$$|\alpha, m\rangle = \frac{(a^+)^m |\alpha\rangle}{\sqrt{\langle\alpha|(a^-)^m (a^+)^m |\alpha\rangle}}, \tag{2}$$

where

$$\langle\alpha|(a^-)^m (a^+)^m |\alpha\rangle = m! L_m(-|\alpha|^2). \tag{3}$$

The Laguerre polynomial $L_m(x)$ of order m is defined by

$$L_m(x) = \sum_{n=0}^{m} \frac{(-1)^n m! x^n}{(n!)^2 (m-n)!}. \tag{4}$$

Photon added coherent states interpolate between coherent states (quasi-classical states) and Fock states and exhibit non-classical features such as squeezing, negativity of Wigner distribution and sub Poissonian statistics. Their experimental generation using parametric down conversion in a nonlinear crystal was reported in [47]. Photon-coherent states are not orthogonal each other. Indeed using the result

$$\langle -\alpha|(a^-)^m(a^+)^m|\alpha\rangle = e^{-2|\alpha|^2} m! L_m(|\alpha|^2), \tag{5}$$

it is simply verified that the overlapping between the states $|\alpha, m\rangle$ and $|-\alpha, m\rangle$ (2) is

$$\langle -\alpha, m|\alpha, m\rangle = e^{-2|\alpha|^2} \frac{L_m(|\alpha|^2)}{L_m(-|\alpha|^2)}. \tag{6}$$

Now, we consider a single mode excitation of the GHZ-type entangled coherent states defined by [23]

$$|\mathrm{GHZ}_k(\alpha)\rangle = \mathcal{C}_k(\alpha)(|\alpha, \alpha, \alpha\rangle + e^{ik\pi}|-\alpha, -\alpha, -\alpha\rangle). \tag{7}$$

where $k \in \mathbb{Z}$ and the normalization constant $\mathcal{C}_k$ is given by

$$\mathcal{C}_k^{-2}(\alpha) = 2 + 2e^{-6|\alpha|^2} \cos k\pi. \tag{8}$$

Mathematically, the m photon excitation process of the first mode, is realized as follows

$$||\mathrm{GHZ}_k(\alpha, m)\rangle = ((a^+)^m \otimes \mathbb{I} \otimes \mathbb{I})\ |\mathrm{GHZ}_k(\alpha)\rangle, \tag{9}$$

from which we introduce the normalized photon added quasi-GHZ coherent states as

$$|\mathrm{GHZ}_k(\alpha, m)\rangle = \frac{||\mathrm{GHZ}_k(\alpha, m)\rangle}{\sqrt{\langle \mathrm{GHZ}_k(\alpha, m)||\mathrm{GHZ}_k(\alpha, m)\rangle}}. \tag{10}$$

In equation (9), $\mathbb{I}$ is the identity operator. Using the expressions (3) and (5), the state (10) rewrites as

$$|\mathrm{GHZ}_k(\alpha, m)\rangle = \mathcal{C}_k(\alpha, m)(|m, \alpha\rangle \otimes |\alpha\rangle \otimes |\alpha\rangle + e^{ik\pi}|m, -\alpha\rangle \otimes |-\alpha\rangle \otimes |-\alpha\rangle). \tag{11}$$

where the normalization factor is

$$\mathcal{C}_k^{-2}(\alpha, m) = 2 + 2\kappa_m e^{-6|\alpha|^2} \cos k\pi, \tag{12}$$

with

$$\kappa_m \equiv \kappa_m(|\alpha|^2) := \frac{L_m(|\alpha|^2)}{L_m(-|\alpha|^2)}. \tag{13}$$

The quantity κ_m (13) goes to unit for $m = 0$ and the state $|\mathrm{GHZ}_k(\alpha, m)\rangle$ (11) reduces to $|\mathrm{GHZ}_k(\alpha)\rangle$ (7). It is also important to note that for $|\alpha|$ large, the overlap between Glauber coherent states $|\alpha\rangle$ and $|-\alpha\rangle$ approaches zero and then they are quasi-orthogonal. In this limiting situation, the state $|\mathrm{GHZ}_k(\alpha)\rangle$ (7) reduces to an usual three qubit state of GHZ-type [24]

$$|\mathrm{GHZ}_k(\infty)\rangle = \frac{1}{\sqrt{3}}(|\mathbf{0}\rangle \otimes |\mathbf{0}\rangle \otimes |\mathbf{0}\rangle + e^{ik\pi}|\mathbf{1}\rangle \otimes |\mathbf{1}\rangle \otimes |\mathbf{1}\rangle). \tag{14}$$

where $|\mathbf{0}\rangle \equiv |\alpha\rangle$ and $|\mathbf{1}\rangle \equiv |-\alpha\rangle$.

2.2 Qubit encoding

To derive the pairwise quantum discord in the three modes system $1-2-3$ described by the state

$$\rho_{123} = |\mathrm{GHZ}_k(\alpha, m)\rangle\langle \mathrm{GHZ}_k(\alpha, m)|,$$

one needs the reduced density matrices corresponding to the two qubit subsystems $1-2$, $2-3$ and $1-3$. It is simple to check that the reduced density matrices $\rho_{12} = \mathrm{Tr}_3\rho_{123}$ and $\rho_{13} = \mathrm{Tr}_2\rho_{123}$ are identical. They write

$$\rho_{12} = \rho_{13} = \frac{\mathcal{C}_k^2(\alpha, m)}{\mathcal{N}_k^2(\alpha, m)}\left[\left(\frac{1+e^{-2|\alpha|^2}}{2}\right)|\mathrm{B}_k(\alpha, m)\rangle\langle \mathrm{B}_k(\alpha, m)| + \left(\frac{1-e^{-2|\alpha|^2}}{2}\right)Z|\mathrm{B}_k(\alpha, m)\rangle\langle \mathrm{B}_k(\alpha, m)|Z\right] \quad (15)$$

where $|\mathrm{B}_k(\alpha, m)\rangle$ are the photon added quasi-Bell states defined by

$$|\mathrm{B}_k(\alpha, m)\rangle = \mathcal{N}_k(\alpha, m)\ \big[|m, \alpha\rangle \otimes |\alpha\rangle + e^{ik\pi}\ |m, -\alpha\rangle \otimes |-\alpha\rangle\big], \quad (16)$$

in terms of the normalized photon added coherent state (2). The factor $\mathcal{N}_k$ is given

$$\mathcal{N}_k^{-2}(\alpha, m) = 2 + 2\kappa_m e^{-4|\alpha|^2}\cos k\pi. \quad (17)$$

where κ_m is defined by (13). The operator Z, in (15), is the third Pauli generator defined by

$$Z|\mathrm{B}_k(\alpha, m)\rangle = \mathcal{N}_k(\alpha, m)[|m, \alpha) \otimes |\alpha\rangle - e^{ik\pi}|m, -\alpha) \otimes |-\alpha\rangle].$$

In the absence of photon excitation ($m = 0$), the states $|\mathrm{B}_k(\alpha, m)\rangle$ (16) reduce to the ordinary quasi-Bell states [22]

$$|\mathrm{B}_k(\alpha)\rangle = \mathcal{N}_k(\alpha, 0)\ \big[|\alpha\rangle \otimes |\alpha\rangle + e^{ik\pi}|-\alpha\rangle \otimes |-\alpha\rangle\big]. \quad (18)$$

Similarly, by tracing out the first mode, the reduced matrix density ρ_{23} takes the form

$$\rho_{23} = \frac{\mathcal{C}_k^2(\alpha, m)}{\mathcal{N}_k^2(\alpha, 0)}\left[\left(\frac{1+\kappa_m e^{-2|\alpha|^2}}{2}\right)|\mathrm{B}_k(\alpha, 0)\rangle\langle \mathrm{B}_k(\alpha, 0)| + \left(\frac{1-\kappa_m e^{-2|\alpha|^2}}{2}\right)Z|\mathrm{B}_k(\alpha, 0)\rangle\langle \mathrm{B}_k(\alpha, 0)|Z\right]. \quad (19)$$

According to [20], the bipartite states ρ_{12}, ρ_{13} and ρ_{23} can be converted in two qubit states by encoding information in even and odd Glauber coherent states (Shrödinger cat states). To realize such encoding scheme, we introduce the following qubit mapping

$$|m, \pm\alpha) = \sqrt{\frac{1+\kappa_m e^{-2|\alpha|^2}}{2}}\ |0\rangle_1 \pm \sqrt{\frac{1-\kappa_m e^{-2|\alpha|^2}}{2}}\ |1\rangle_1 \quad (20)$$

for the first mode. For the second and third modes, we consider the logical qubits defined by

$$|\pm\alpha\rangle = \sqrt{\frac{1+e^{-2|\alpha|^2}}{2}}\ |0\rangle_i \pm \sqrt{\frac{1-e^{-2|\alpha|^2}}{2}}\ |1\rangle_i \qquad i = 2, 3 \quad (21)$$

Substituting (20) and (21) in (15) (resp. (19)), one can express the density matrix $\rho_{12} = \rho_{13}$ (resp. ρ_{23}) in the two qubit basis $\{|0\rangle_1 \otimes |0\rangle_2, |0\rangle_1 \otimes |1\rangle_2, |1\rangle_1 \otimes |0\rangle_2, |1\rangle_1 \otimes |1\rangle_2\}$ (resp. $\{|0\rangle_2 \otimes |0\rangle_3, |0\rangle_2 \otimes$

$|1\rangle_3, |1\rangle_2 \otimes |0\rangle_3, |1\rangle_2 \otimes |1\rangle_3\}$). One can verify that the density matrices ρ_{12}, ρ_{13} and ρ_{23} have non vanishing entries only along the diagonal and the anti-diagonal. They resemble to the alphabet X and thus belong to the family of so called X-states that have been of interest in a variety of contexts in the field of quantum information [48].

As the main of this paper concerns the monogamy property of geometric discord in the state $|\mathrm{GHZ}_k(\alpha, m)\rangle$, we consider the bipartition of the state (11) in which the modes 2 and 3 are grouped in a single qubit. For the first mode, the information is encoded in the logical qubits $\{|0\rangle_1, |1\rangle_1\}$ (20) given by defined by

$$|0\rangle_1 = \frac{|m,\alpha\rangle + |m,\alpha\rangle}{\sqrt{2(1+\kappa_m e^{-2|\alpha|^2})}} \qquad |1\rangle_1 = \frac{|m,\alpha\rangle - |m,\alpha\rangle}{\sqrt{2(1-\kappa_m e^{-|\alpha|^2})}}. \tag{22}$$

For the modes (23), viewed as a single subsystem, we introduce the orthogonal basis $\{|0\rangle_{23}, |1\rangle_{23}\}$ as follows

$$|0\rangle_{23} = \frac{|\alpha,\alpha\rangle + |-\alpha,-\alpha\rangle}{\sqrt{2(1+e^{-4|\alpha|^2})}} \qquad |1\rangle_{23} = \frac{|\alpha,\alpha\rangle - |-\alpha,-\alpha\rangle}{\sqrt{2(1-e^{-4|\alpha|^2})}}. \tag{23}$$

Inserting(22) and (23) in $|\mathrm{GHZ}_k(\alpha, m)\rangle$, one obtains the expansion of the pure state $|\mathrm{GHZ}_k(\alpha, m)\rangle$ in the basis $\{|0\rangle_1 \otimes |0\rangle_{23}, |0\rangle_1 \otimes |1\rangle_{23}, |1\rangle_1 \otimes |0\rangle_{23}, |1\rangle_1 \otimes |1\rangle_{23}\}$. Explicitly, one has

$$|\mathrm{GHZ}_k(\alpha, m)\rangle = \sum_{\alpha=0,1} \sum_{\beta=0,1} C_{\alpha,\beta} |\alpha\rangle_1 \otimes |\beta\rangle_{23} \tag{24}$$

where the coefficients $C_{\alpha,\beta}$ are

$$C_{0,0} = \mathcal{C}_k(\alpha, m)(1+e^{ik\pi})c_1^+ c_{23}^+, \qquad C_{0,1} = \mathcal{C}_k(\alpha, m)(1-e^{ik\pi})c_1^+ c_{23}^-$$

$$C_{1,0} = \mathcal{C}_k(\alpha, m)(1-e^{ik\pi})c_{23}^+ c_1^-, \qquad C_{1,1} = \mathcal{C}_k(\alpha, m)(1+e^{ik\pi})c_1^- c_{23}^-.$$

in terms of the quantities

$$c_1^\pm = \sqrt{\frac{1 \pm \kappa_m e^{-2|\alpha|^2}}{2}} \qquad c_{23}^\pm = \sqrt{\frac{1 \pm e^{-4|\alpha|^2}}{2}}.$$

It is interesting to note that using the Schmidt decomposition, one can shows that the density matrix

$$\rho_{123} \equiv \rho_{1|23} = |\mathrm{GHZ}_k(\alpha, m)\rangle\langle \mathrm{GHZ}_k(\alpha, m)| \tag{25}$$

is also X shaped. This point will be clarified in the following subsection.

2.3 Fano-Bloch representations

By encoding information in the qubits (20) (21) and (23), the arising density matrices $\rho_{12} = \rho_{23}$ (15) and $\rho_{1|23}$ (25) take, in Fano-Bloch representation, the following form

$$\rho_{AB} = \frac{1}{4}\Big[\sigma_0 \otimes \sigma_0 + T_{03}^{AB}\ \sigma_0 \otimes \sigma_3 + T_{30}^{AB}\ \sigma_3 \otimes \sigma_0 + \sum_{k=1,2,3} T_{kk}^{AB}\ \sigma_k \otimes \sigma_k\Big] \tag{26}$$

where σ_0 is the identity, σ_k are the Pauli matrices and the correlation matrix elements are given by

$$T_{\alpha\beta}^{AB} = \mathrm{Tr}\big(\rho_{AB}\ \sigma_\alpha \otimes \sigma_\beta\big).$$

Explicitly, the correlation matrix elements entering in Fano-Bloch expression of the bipartite density matrix $\rho_{12} = \mathrm{Tr}_3\rho_{123}$ (15) write as

$$
\begin{aligned}
T_{03}^{12} &= 2\mathcal{C}_k^2(\alpha,m)\ (e^{-2|\alpha|^2} + \kappa_m e^{-4|\alpha|^2}\cos k\pi)\\
T_{30}^{12} &= 2\mathcal{C}_k^2(\alpha,m)\ (\kappa_m e^{-2|\alpha|^2} + e^{-4|\alpha|^2}\cos k\pi)\\
T_{11}^{12} &= 2\mathcal{C}_k^2(\alpha,m)\ \sqrt{(1-\kappa_m^2 e^{-4|\alpha|^2})(1-e^{-4|\alpha|^2})}\\
T_{22}^{12} &= -2\mathcal{C}_k^2(\alpha,m)\ \sqrt{(1-\kappa_m^2 e^{-4|\alpha|^2})(1-e^{-4|\alpha|^2})}\ e^{-2|\alpha|^2}\cos k\pi\\
T_{33}^{12} &= 2\mathcal{C}_k^2(\alpha,m)\ (\kappa_m e^{-4|\alpha|^2} + e^{-2|\alpha|^2}\cos k\pi)
\end{aligned}
\tag{27}
$$

Similarly, for ρ_{23} (19) one obtains

$$
\begin{aligned}
T_{03}^{23} &= 2\mathcal{C}_k^2(\alpha,m)\ (e^{-2|\alpha|^2} + \kappa_m e^{-4|\alpha|^2}\cos k\pi)\\
T_{30}^{23} &= 2\mathcal{C}_k^2(\alpha,m)\ (e^{-2|\alpha|^2} + \kappa_m e^{-4|\alpha|^2}\cos k\pi)\\
T_{11}^{23} &= 2\mathcal{C}_k^2(\alpha,m)(1-e^{-4|\alpha|^2})\\
T_{22}^{23} &= 2\mathcal{C}_k^2(\alpha,m)(1-e^{-4|\alpha|^2})\kappa_m e^{-2|\alpha|^2}\cos k\pi\\
T_{33}^{23} &= 2\mathcal{C}_k^2(\alpha,m)\ (e^{-4|\alpha|^2} + \kappa_m e^{-2|\alpha|^2}\cos k\pi)
\end{aligned}
\tag{28}
$$

Using the Schmidt decomposition, the state (24) rewrites as

$$
|\mathrm{GHZ}_k(\alpha,m)\rangle_{1|23} = \sqrt{\lambda_+}|+\rangle_1 \otimes |+\rangle_{23} + \sqrt{\lambda_-}|-\rangle_1 \otimes |-\rangle_{23} \tag{29}
$$

where $|\pm\rangle_1$ (resp. $|\pm\rangle_{23}$) denotes the eigenvectors of the reduced density matrix ρ_1 (resp. ρ_{23} viewed as a single qubit state). The Schmidt eigenvalues λ_+ and λ_- are given by

$$
\lambda_\pm = \frac{1}{2}\left[1 \pm e^{-2|\alpha|^2}\,\frac{\kappa_m + e^{-2|\alpha|^2}\cos k\pi}{1+\kappa_m e^{-6|\alpha|^2}\cos k\pi}\right]. \tag{30}
$$

In the basis $\{|+\rangle_1 \otimes |+\rangle_{23}, |+\rangle_1 \otimes |-\rangle_{23}, |-\rangle_1 \otimes |+\rangle_{23}, |-\rangle_1 \otimes |-\rangle_{23}\}$, the density $\rho_{1|23}$ (25) is X shaped and takes the form (26). The associated correlation matrix elements are given by

$$
\begin{aligned}
T_{33}^{1|23} &= 1\\
T_{03}^{1|23} = T_{30}^{1|23} &= 2\mathcal{C}_k^2(\alpha,m)e^{-2|\alpha|^2}(\kappa_m + e^{-2|\alpha|^2}\cos k\pi)\\
T_{11}^{1|23} = -T_{22}^{1|23} &= 2\mathcal{C}_k^2(\alpha,m)\sqrt{(1-\kappa_m^2 e^{-4|\alpha|^2})(1-e^{-8|\alpha|^2})}.
\end{aligned}
\tag{31}
$$

3 Geometric quantum discord in photon added coherent states

3.1 Hilbert-Schmidt measure of quantum discord

The qubit encoding introduced in the previous section is of paramount importance in deriving the geometric quantum discord in photon added coherent states (11) and analyzing the influence of the photon excitation process. According to the procedure developed in [31], the geometric measure of quantum discord is the distance between the state ρ_{AB} and its closest classical-quantum state presenting zero discord

$$D_{AB} = \min_{\chi_{AB}} ||\rho_{AB} - \chi_{AB}||^2 \tag{32}$$

where the Hilbert-Schmidt norm is defined by $||X||^2 = \mathrm{Tr}(X^\dagger X)$ and the minimization is taken over the set of all classical states. When the measurement is performed on the qubit A, the classical states write

$$\chi_{AB} = p_1|\psi_1\rangle\langle\psi_1| \otimes \rho_1^B + p_2|\psi_2\rangle\langle\psi_2| \otimes \rho_2^B \tag{33}$$

where $\{|\psi_1\rangle, |\psi_2\rangle\}$ is an orthonormal basis related to the qubit A, p_i $(i = 1, 2)$ stands for probability distribution and ρ_i^B $(i = 1, 2)$ is the marginal density of the qubit B. The classically correlated states χ_{AB} can also be written as

$$\chi_{AB} = \frac{1}{4}\left[\sigma_0 \otimes \sigma_0 + \sum_{i=1}^{3} te_i \;\; \sigma_i \otimes \sigma_0 + \sum_{i=1}^{3}(s_+)_i \; \sigma_0 \otimes \sigma_i + \sum_{i,j=1}^{3} e_i(s_-)_j \; \sigma_i \otimes \sigma_j\right] \tag{34}$$

where

$$t = p_1 - p_2, \qquad e_i = \langle\psi_1|\sigma_i|\psi_1\rangle, \qquad (s_\pm)_j = \mathrm{Tr}\big((p_1\rho_1^B \pm p_2\rho_2^B)\sigma_j\big).$$

It follows that the distance between the density matrix ρ_{AB} and the classical state χ_{AB}, as measured by Hilbert-Schmidt norm, is then given by

$$||\rho_{AB} - \chi_{AB}||^2 = \frac{1}{4}\left[(t^2 - 2te_3T_{30}^{AB} + \big(T_{30}^{AB}\big)^2) + \sum_{i=1}^{3}(T_{0i}^{AB} - (s_+)_i)^2 + \sum_{i,j=1}^{3}(T_{ij}^{AB} - e_i(s_-)_j)^2\right]. \tag{35}$$

The minimization of the distance (35), with respect to the parameters t, $(s_+)_i$ and $(s_-)_i$, gives

$$t = e_3T_{30}^{AB}, \qquad (s_-)_i = \sum_{j=1}^{3} e_jT_{ji}^{AB},$$

$$(s_+)_1 = (s_+)_2 = 0, \qquad (s_+)_3 = T_{03}^{AB}. \tag{36}$$

Inserting the solutions (36) in (35), one has

$$||\rho_{AB} - \chi_{AB}||^2 = \frac{1}{4}\left[\mathrm{Tr}K - \vec{e}^{\,t}K\vec{e}\right] \tag{37}$$

where the diagonal matrix K is defined by

$$K = \mathrm{diag}\big(\lambda_1^{AB}, \lambda_2^{AB}, \lambda_3^{AB}\big) \tag{38}$$

with

$$\lambda_1^{AB} = \left(T_{11}^{AB}\right)^2, \quad \lambda_2^{AB} = \left(T_{22}^{AB}\right)^2, \qquad \lambda_3^{AB} = \left(T_{30}^{AB}\right)^2 + (T_{33}^{AB})^2. \tag{39}$$

From the expressions (27), we obtain the eigenvalues

$$\begin{aligned}
\lambda_1^{12} &= \frac{(1-\kappa_m^2 e^{-4|\alpha|^2})(1-e^{-4|\alpha|^2})}{(1+\kappa_m e^{-6|\alpha|^2}\cos k\pi)^2}, \\
\lambda_2^{12} &= e^{-4|\alpha|^2}\ \frac{(1-\kappa_m^2 e^{-4|\alpha|^2})(1-e^{-4|\alpha|^2})}{(1+\kappa_m e^{-6|\alpha|^2}\cos k\pi)^2}, \\
\lambda_3^{12} &= e^{-4|\alpha|^2}\ \frac{(1+\kappa_m^2)(1+e^{-4|\alpha|^2}) + 4\kappa_m e^{-2|\alpha|^2}\cos k\pi}{(1+\kappa_m e^{-6|\alpha|^2}\cos k\pi)^2}.
\end{aligned} \tag{40}$$

corresponding to the state ρ_{12}. Reporting (28) in (39), the eigenvalues entering in the determination of the bipartite geometric quantum discord in the state ρ_{23} are

$$\begin{aligned}
\lambda_1^{23} &= \left(\frac{1-e^{-4|\alpha|^2}}{1+\kappa_m e^{-6|\alpha|^2}\cos k\pi}\right)^2, \\
\lambda_2^{23} &= \kappa_m^2 e^{-4|\alpha|^2}\ \left(\frac{1-e^{-4|\alpha|^2}}{1+\kappa_m e^{-6|\alpha|^2}\cos k\pi}\right)^2, \\
\lambda_3^{23} &= e^{-4|\alpha|^2}\ \frac{(1+\kappa_m^2)(1+e^{-4|\alpha|^2}) + 4\kappa_m e^{-2|\alpha|^2}\cos k\pi}{(1+\kappa_m e^{-6|\alpha|^2}\cos k\pi)^2}.
\end{aligned} \tag{41}$$

For the pure state $\rho_{1|23}$, we use the expressions (31) to obtain

$$\begin{aligned}
\lambda_1^{1|23} &= \frac{(1-\kappa_m^2 e^{-4|\alpha|^2})(1-e^{-8|\alpha|^2})}{(1+\kappa_m e^{-6|\alpha|^2}\cos k\pi)^2}, \\
\lambda_2^{1|23} &= \frac{(1-\kappa_m^2 e^{-4|\alpha|^2})(1-e^{-8|\alpha|^2})}{(1+\kappa_m e^{-6|\alpha|^2}\cos k\pi)^2}, \\
\lambda_3^{1|23} &= 2 - \frac{(1-\kappa_m^2 e^{-4|\alpha|^2})(1-e^{-8|\alpha|^2})}{(1+\kappa_m e^{-6|\alpha|^2}\cos k\pi)^2}.
\end{aligned} \tag{42}$$

From the equation (37), it is clear that the minimal value of Hilbert-Schmidt distance is reached for the largest eigenvalue of the matrix K (38). Hence, to get the minimal value of the Hilbert-Schmidt distance (37) and subsequently the amount of geometric quantum discord, one should compare λ_1^{AB}, λ_2^{AB} and λ_3^{AB}. From the results (40), (41) and (42), it is simply verified that λ_1^{AB} is always greater than λ_2^{AB}. This implies that the largest eigenvalue $\lambda_{\max}^{AB}$ is λ_1^{AB} or λ_3^{AB}. Accordingly, the geometric discord is given by

$$D_{AB} = \frac{1}{4}\ \min\{\lambda_1^{AB} + \lambda_2^{AB}, \lambda_2^{AB} + \lambda_3^{AB}\}. \tag{43}$$

To write down the explicit expressions of the closest classical state χ_{AB} to ρ_{AB}, one has to determine the eigenvector $\vec{e}_{\max}$ associated with the largest eigenvalue $\lambda_{\max}$. In this respect, two cases ($\lambda_{\max} = \lambda_1$ and $\lambda_{\max} = \lambda_3^{AB}$) are separately discussed. In the case where $\lambda_{\max} = \lambda_1^{AB}$, the corresponding eigenvector is given by $\vec{e}_1 = (1,0,0)$ and using (36), one gets the closest classical state

$$\chi_{AB}^1 = \frac{1}{4}\left[\sigma_0\otimes\sigma_0 + T_{30}^{AB}\ \ \sigma_3\otimes\sigma_0 + T_{11}^{AB}\ \sigma_1\otimes\sigma_1\right] \tag{44}$$

In the second situation where $\lambda_{\max} = \lambda_3^{AB}$, the associated eigenvector is given by $\vec{e}_3 = (0, 0, 1)$. Reporting this result in the set of constraints (36), one shows

$$\chi_{AB}^3 = \frac{1}{4}\Big[\sigma_0 \otimes \sigma_0 + T_{30}^{AB}\ \ \sigma_3 \otimes \sigma_0 + T_{03}^{AB}\ \sigma_0 \otimes \sigma_3 + T_{33}^{AB}\ \sigma_3 \otimes \sigma_3\Big] \tag{45}$$

3.2 Pairwise geometric discord in tripartite quasi-GHZ coherent states

To analyze the influence of the photon excitation on the pairwise geometric discord present in the state (11), we consider first the evolution of the correlation between the first and the second mode described by the state (15). From equation (43), we have

$$D_{12} = \frac{1}{4}\ (\lambda_2^{12} + \min\{\lambda_1^{12}, \lambda_3^{12}\}). \tag{46}$$

where $\lambda_i^{12} (i = 1, 2, 3)$ are given by (40). The behavior of D_{12} in (46) is plotted, in figures 1 and 2, as function of $|\alpha|^2$ for different values of photon excitation order m. In figure 1, corresponding to symmetric case, it is clearly seen that the geometric quantum discord D_{12} exhibits a pick. This pick is moving from the right to the left. In particular, the height of the pick, reflecting the maximal amount of quantum discord, increases as the photon excitation order m increases. Also, the photon excitation induces a quick decreases of quantum discord as the optical strength $|\alpha|$ becomes large. For antisymmetric states ($k = 1$), the quantum discord D_{12}, depicted in figure 2, shows that the quantum discord corresponding to $m = 0, 1, 2$ does not present peak and it decreases monotonically as $|\alpha|$ increases. This is not the case for $m \geq 3$. In fact, the geometric discord starts increasing to reach a maximal value for α, different from zero, to decrease after quickly as the Glauber coherent state amplitude becomes large. It must be noticed that for symmetric as well as antisymmetric states the quantum discord D_{12} vanishes when $\alpha \to \infty$ independently of photon excitation number m. This limiting case corresponds to usual GHZ states (14). Another interesting limiting case concerns the antisymmetric states $|\mathrm{GHZ}_1(\alpha, m)\rangle$ when $|\alpha| \to 0$. In this case, it simply verified that the state (11) reduces to

$$|\mathrm{GHZ}_1(0, m)\rangle = \frac{1}{\sqrt{m+3}}(\sqrt{m+1}|m+1, 0, 0\rangle + |m, 1, 0\rangle + |m, 0, 1\rangle) \tag{47}$$

which coincides with the three qubit W states for $m = 0$ [49]. In this limit the first qubit is encoded in the Fock states $|m\rangle$ and $|m+1\rangle$ and the two other modes are encoded in the states $|0\rangle$ and $|1\rangle$. In the limit $|\alpha| \longrightarrow 0$, the Laguerre function (4) behaves like $L_m(|\alpha|^2) \simeq 1 - m|\alpha|^2$ and the quantity κ_m (13) writes

$$\kappa_m \simeq 1 - 2m|\alpha|^2. \tag{48}$$

It follows that the eigenvalues (40) reduce to

$$\lambda_1^{12} \longrightarrow 4\ \frac{m+1}{(m+3)^2}, \quad \lambda_2^{12} \longrightarrow 4\ \frac{m+1}{(m+3)^2}, \quad \lambda_3^{12} \longrightarrow 2\ \frac{m^2+1}{(m+3)^2}. \tag{49}$$

This shows that the quantum discord D_{12} is m-dependent for states of W-type (47) and one has

$$D_{12} \longrightarrow \frac{(m+1)^2+2}{2(m+3)^2} \quad \text{for} \quad m \leq 2$$

$$D_{12} \longrightarrow 2\,\frac{m+1}{(m+3)^2} \quad \text{for} \quad m > 2.$$

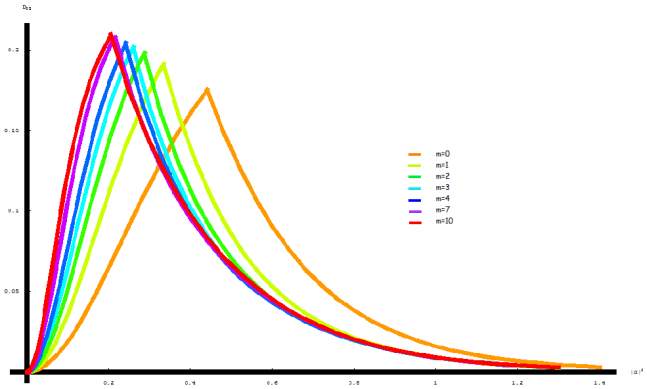

Figure 1. The quantum discord D_{12} versus $|\alpha|^2$ for $k = 0$ and different values of photon excitation number m.

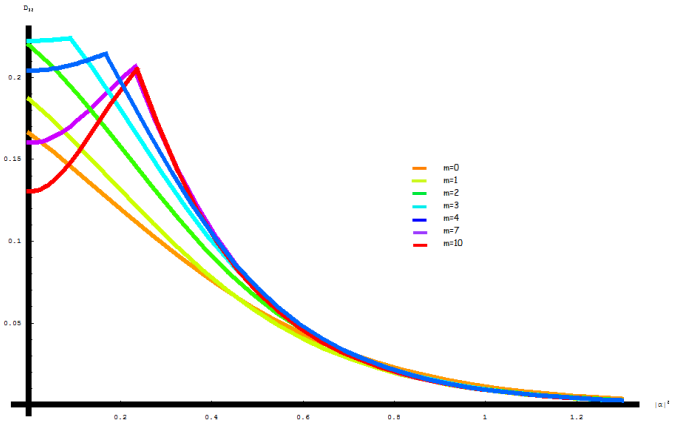

Figure 2. The quantum discord D_{12} versus $|\alpha|^2$ for $k = 1$ and different values of photon excitation number m.

In the subsystem described by the density matrix (19), the quantum discord (43) gives

$$D_{23} = \frac{1}{4}\,(\lambda_2^{23} + \min\{\lambda_1^{23}, \lambda_3^{23}\}). \tag{50}$$

where $\lambda_i^{23} (i = 1, 2, 3)$ are given by (41). In the figures 3 and 4 are depicted the geometric measures of quantum correlation between the modes 2 and 3 in the states $|\mathrm{GHZ}_k(\alpha, m)\rangle$ (11) as function of $|\alpha|^2$. From figure 3, one observes that the height of the quantum discord D_{23} diminishes as the photon excitation order m increases, contrarily to what happens with the pairwise quantum discord D_{12} (figure 1). The peaks move from the right to the left. In increasing the number of added photons, D_{23} becomes almost identical. The behavior of D_{23} for symmetric states (figure 3) is different from one in the antisymmetric states (figure 4). In particular, the quantum discord decreases monotonically for

$m \leq 1$. The first peak appears for $m = 2$ and it moves to the right for $m \geq 3$. The quantum discord vanishes quickly, as $|\alpha|$ increases, under the effect of photon excitation. The quantum discord D_{23}, in antisymmetric states ($k = 1$), depends on the photon excitation order m when $|\alpha|$ approaches zero. Indeed, from equations (41), one shows that

$$\lambda_1^{23} \longrightarrow \frac{4}{(m+3)^2}, \qquad \lambda_2^{23} \longrightarrow \frac{4}{(m+3)^2}, \qquad \lambda_3^{23} \longrightarrow 2\,\frac{m^2+1}{(m+3)^2}, \tag{51}$$

and subsequently one obtains the results

$$D_{23} \longrightarrow \frac{m^2+3}{2(m+3)^2} \quad \text{for} \quad m \leq 2$$

$$D_{23} \longrightarrow \frac{2}{(m+3)^2} \quad \text{for} \quad m > 2$$

which give the amount of pairwise quantum discord between the modes 2 and 3 in the photon added W states (47) and confirms analytically the results reported in the figure 4.

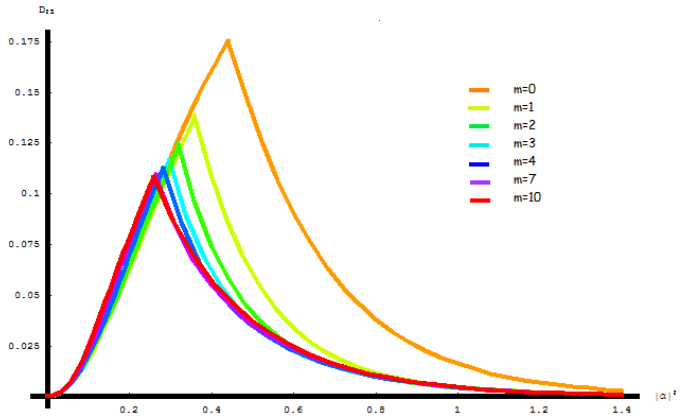

Figure 3. The quantum discord D_{23} versus $|\alpha|^2$ for $k = 0$ and different values of photon excitation number m.

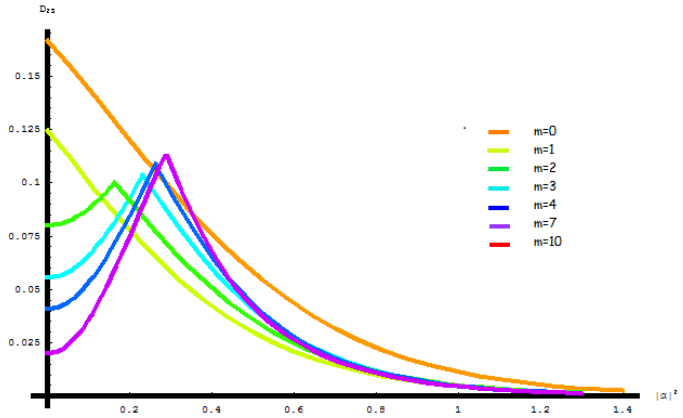

Figure 4. The quantum discord D_{23} versus $|\alpha|^2$ for $k = 1$ and different values of photon excitation number m.

Finally, we discuss the evolution of $D_{1|23}$ in the bi-partitioning scheme (25). From (42) it is simple to verify that the maximal eigenvalue is $\lambda_3^{1|23}$. Thus, the quantum geometric measure of quantum discord

between the first qubit and the qubit grouping the modes 2 and 3 is given by

$$D_{1|23} = \frac{1}{2}\frac{(1-\kappa_m^2 e^{-4|\alpha|^2})(1-e^{-8|\alpha|^2})}{(1+\kappa_m e^{-6|\alpha|^2}\cos k\pi)^2}. \tag{52}$$

The behavior of $D_{1|23}$ versus $|\alpha|^2$ for symmetric GHZ states for different values of added photons is reported in figure 5. In the weak regime, the geometric quantum discord increases quickly as m increases. For high values of $|\alpha|$, one obtain $D_{1|23} = 0.5$ independently of m. This result is easily verified from (52). Similar behavior, when $|\alpha|$ is large, is obtained with antisymmetric GHZ states (see figure 6). From figure 6, it is clearly seen that in the weak regime, the pairwise quantum $D_{1|23}$ is strongly influenced by the photon excitation. In particular, when $|\alpha| \to 0$, the eigenvalues (42) become

$$\lambda_1^{1|23} \longrightarrow 8\,\frac{m+1}{(m+3)^2}, \qquad \lambda_2^{1|23} \longrightarrow 8\,\frac{m+1}{(m+3)^2}, \qquad \lambda_3^{1|23} \longrightarrow 2-8\,\frac{m+1}{(m+3)^2}, \tag{53}$$

and the explicit expression of quantum discord $D_{1|23}$ as function of m is

$$D_{1|23} \quad \longrightarrow \quad 4\,\frac{m+1}{(m+3)^2}. \tag{54}$$

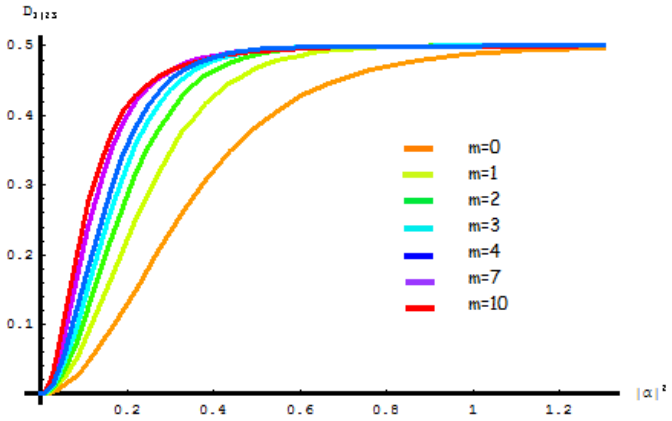

Figure 5. The quantum discord $D_{1|23}$ versus $|\alpha|^2$ for $k = 0$ and different values of photon excitation number m.

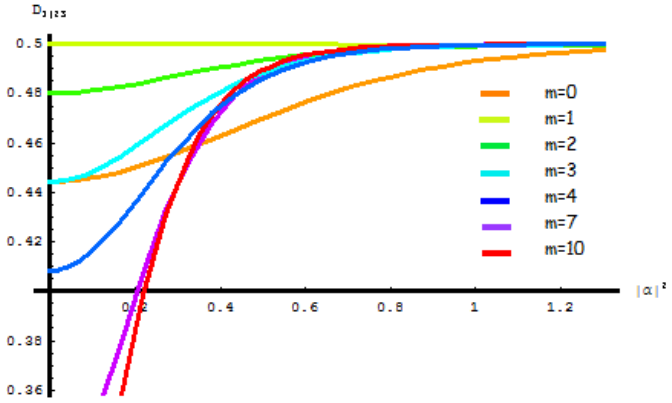

Figure 6. The quantum discord $D_{1|23}$ versus $|\alpha|^2$ for $k = 1$ and different values of photon excitation number m.

3.3 Monogamy of geometric quantum discord in quasi-GHZ states

The quantum discord, in the states $|\mathrm{GHZ}_k(\alpha, m)\rangle$ (11), is monogamous if and only if the quantum monogamy deficit defined by

$$\Delta_{123} = \Delta_{123}(m, |\alpha|^2) = D_{1|23} - D_{12} - D_{13}, \tag{55}$$

is positive. In other words, the monogamy property is satisfied when the quantum discord $D_{1|23}$ (52) between the first mode and the modes 2-3 (viewed as a single subsystem) exceeds the sum of pairwise quantum discord D_{12} and D_{13} (46). Using (40) and (46), one shows that

$$D_{12} = D_{13} = \frac{1}{4}\,\frac{(1-\kappa_m^2 e^{-4|\alpha|^2})(1-e^{-8|\alpha|^2})}{(1+\kappa_m e^{-6|\alpha|^2}\cos k\pi)^2}, \tag{56}$$

when $\lambda_1^{12} \leq \lambda_3^{12}$. Conversely, for photon excitation order m and optical strength $|\alpha|$ satisfying the condition $\lambda_1^{12} \geq \lambda_3^{12}$, one gets

$$D_{12} = D_{13} = \frac{1}{4}\, e^{-4|\alpha|^2}\,\frac{2+\kappa_m^2 e^{-8|\alpha|^2} + 4\kappa_m e^{-2|\alpha|^2}\cos k\pi}{(1+\kappa_m e^{-6|\alpha|^2}\cos k\pi)^2}. \tag{57}$$

Using the expressions (52), (56) and (57), it is easy to check that the quantum monogamy deficit (55) vanishes

$$\Delta_{123} = 0, \tag{58}$$

for $\lambda_1^{12} \leq \lambda_3^{12}$ and it is given by

$$\Delta_{123} = \frac{1}{2}\,\frac{1-\left[(2-3\kappa_m^2) + (e^{-2|\alpha|^2} + 2\kappa_m\cos k\pi)^2\right]e^{-4|\alpha|^2}}{(1+\kappa_m e^{-6|\alpha|^2}\cos k\pi)^2}, \tag{59}$$

when $\lambda_1^{12} \geq \lambda_3^{12}$.

The quantum discord deficit is depicted in figures 7 and 8. It is always positive reflecting that the geometric quantum discord is monogamous. In figure 7 corresponding to the symmetric states ($k = 0$), Δ_{123} is initially zero (see equation (58)) reflecting that the condition $\lambda_1^{12} \leq \lambda_3^{12}$ is satisfied. By increasing the optical strength $|\alpha|$, λ_1^{12} becomes greater than λ_3^{12} and the quantum discord deficit increases to reach its maximal value 0.5 for $|\alpha|$ large. In this situation, it is intersecting to note that, according to the equation (57), $D_{12} = D_{13}$ vanishes and Δ_{123} coincides with the pairwise quantum discord $D_{1|23}$ independently of photon excitation order m.

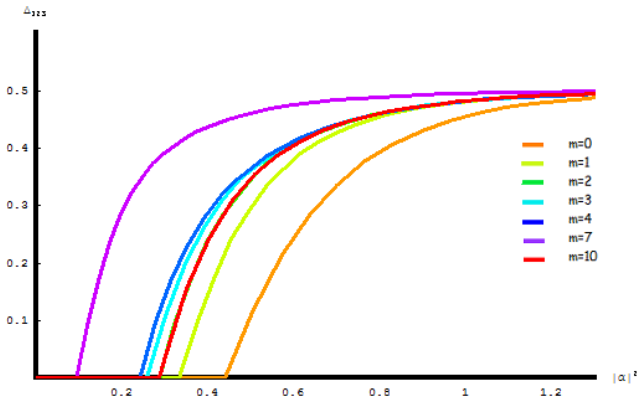

Figure 7. The geometric quantum discord deficit Δ_{123} versus $|\alpha|^2$ for $k = 0$ and different values of photon excitation number m.

It is clearly seen from figure 8 that the quantum discord deficit is non zero for $m = 0, 1, 2$, in particular when $|\alpha| \longrightarrow 0$ in contrast with the states with $m \geq 3$. This result can be confirmed analytically. Indeed, when $|\alpha|$ approaches zero, the antisymmetric states (11) reduces to photon added tripartite states of W-type (47) and using the results (49) and (53), the geometric quantum discord deficit Δ_{123} tends to zero for $m > 2$ and

$$\Delta_{123} \longrightarrow \frac{2-(m-1)^2}{(m+3)^2}$$

for $m = 0, 1, 2$. The photon addition process does not affect the monogamy property (Δ_{123} is positive for any value of m), but modifies the distribution of geometric quantum discord among the three modes in the states (11). In fact, in the case when $m \geq 3$ and for small values of $|\alpha|$, one have $\Delta_{123} = 0$ reflecting that the geometric discord $D_{1|23}$ is exactly the sum of the pairwise quantum correlations D_{12} and D_{13} in contrast with the cases where $m \leq 2$ for which we have $\Delta_{123} > 0$ for any value of $|\alpha|$.

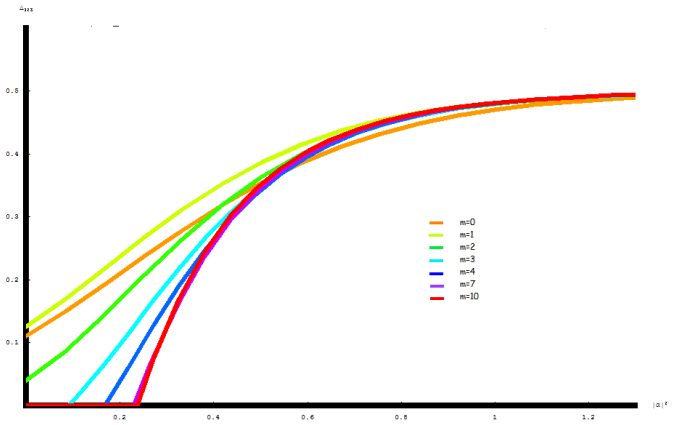

Figure 8. The geometric quantum discord deficit Δ_{123} versus $|\alpha|^2$ for $k = 1$ and different values of photon excitation number m.

4 Concluding remarks

In conclusion, we have addressed the question of the influence of photon excitation on pairwise quantum correlations in balanced superpositions of tripartite Glauber coherent states of type GHZ. This family of nonorthogonal states include Greenberger-Horne-Zeilinger and W states. By encoding information in even and odd coherent states, we derived the pairwise quantum discord D_{12} (46), D_{23} (50) and $D_{1|23}$ (52). We have used the Hilbert-Schmidt distance as quantifier of quantum correlations. We have analyzed their behaviors as functions of the coherent states amplitude α. A special attention were devoted to photon added states of W type corresponding to the limiting case $\alpha \longrightarrow 0$ for which the explicit expressions of the pairwise geometric discord are derived. We have shown that the photon excitation does not affect the monogamy property of geometric quantum discord in the quasi-GHZ states (11). But, it modifies the distribution of quantum discord among the three optical modes,

especially when the Glauber coherent states have small amplitudes. Finally, as prolongation of this work, we think that it would be interesting to analyze the distribution of quantum correlations in photon added coherent states comprising four or more modes. We hope to report on this issue in a forthcoming work.

References

[1] B.C. Sanders, J. Phys. A: Math. Theor. **45** (2012) 244002.

[2] S.J. van Enk and O. Hirota, Phys. Rev. A **64** (2001) 022313.

[3] C.H. Bennett, G. Brassard, C. Crépeau, R. Jozsa, A. Peres and W.K. Wootters , Phys. Rev. Lett. **70** (1993) 1895.

[4] T.J. Johnson, S.D. Bartlett and B.C. Sanders, Phys. Rev. A **66** (2002) 042326.

[5] X. Wang, Phys. Rev. A **64** (2001) 022302.

[6] J. Janszky, A. Gabris, M. Koniorczyk, A. Vukics and J.K. Asbóth, J. Opt. B, Quantum Semiclass. Opt.**4** (2002) S213.

[7] H. Jeong, M.S. Kim and J. Lee, Phys. Rev. A **64** (2001) 052308.

[8] P. van Loock, N. Lütkenhaus, W.J. Munro and K. Nemoto, Phys. Rev. A **78** (2008) 062319.

[9] P.T. Cochrane, G.J. Milburn and W.J. Munro, Phys. Rev. A **59** (1999) 2631.

[10] M.C. de Oliveira and W.J. Munro, Phys. Rev. A **61** (2000) 042309.

[11] H. Jeong and M.S. Kim, Phys. Rev. A **65** (2002) 042305.

[12] N.A. Ansari, L.D. Fiore, M.A. Man'ko and V.I. Man'ko, S. Solimeno and F. Zaccaria, Phys. Rev. A **49** (1994) 2151.

[13] J. Joo, W.J. Munro and T.P. Spiller, Phys. Rev. Lett. **107** (2011) 083601.

[14] H. Jeong and N.B. An, Phys. Rev. A **74** (2006) 022104.

[15] H.M. Li, H.C. Yuan and H.Y. Fan, Int. J. Theor. Phys.**48** (2009) 2849.

[16] N.B. An, K. Kim and J. Kim, Quantum Inf. Comp. **11** (2011) 124

[17] W.J. Munro, G.J. Milburn and B.C. Sanders, Phys. Rev. A **62** (2000) 052108.

[18] L.M. Kuang and L. Zhou, Phys. Rev. A **68** (2003) 043606.

[19] L.M. Kuang, Z.B. Chen and J.W. Pan, Phys. Rev. A **76** (2007) 052324.

[20] T.C. Ralph, A. Gilchrist, J. Milburn, W.J. Munro and S. Glancy, Phys. Rev. A 68, 042319 (2003).

[21] X. Wang and B.C. Sanders, Phys. Rev. A **65** (2001) 012303.

[22] B.C. Sanders, Phys. Rev. A 45 (1992) 6811.

[23] H. Jeong and B.A. Nguyen, Phys. Rev. A **74** (2006) 022104.

[24] D.M. Greenberger, M.A. Horne and A. Zeilinger,*Bell's theorem, Quantum theory and Conceptions of the the Universe* edited by M. Kafatos, Kluwer, Dordrecht (1989) 69.

[25] L. Henderson and V. Vedral, J. Phys. A. Math. Gen. **34** (2001) 6899.

[26] H. Ollivier and W. Zurek, Phys. Rev. Lett. **88** (2002) 017901.

[27] M. Daoud and R. Ahl Laamara, J. Phys. A: Math. Theor. **45** (2012) 325302.

[28] M. Daoud and R. Ahl Laamara, Int. J. Quant. Inf. **10** (2012) 1250060.

[29] M. Daoud, R. Ahl Laamara and W. Kaydi, J. Phys. A: Math. Theor. **46** (2013) 395302.

[30] M Daoud, R Ahl Laamara, R Essaber and W Kaydi, Phys. Scr. **89** (2014) 065004.

[31] B. Dakic, V. Vedral and C. Brukner, phys. Rev. Lett. **105** (2010) 190502.

[32] X. Yin, Z. Xi, X-M Lu, Z. Sun and X. Wang, J. Phys. B: At. Mol. Opt. Phys. **44** (2011) 245502

[33] M. Daoud and R. Ahl Laamara, Int. J. Quant. Inf. **376** (2012) 2361.

[34] L. Xu and L-M Kuang, J. Phys. A: Math. Gen. **39** (2006) L191.

[35] H-C Yuan and L-Y Hu, J. Phys. A: Math. Theor. **43** (2010) 018001.

[36] H-M Li, H-C Yuan and H-Y Fan, Inter. J. Theor. Phys, **48** (2009) 2849.

[37] W.K. Wootters, Phys. Rev. Lett. **80** (1998) 2245.

[38] V. Coffman, J. Kundu and W.K. Wootters, Phys. Rev. A **61** (2000) 052306.

[39] T.J. Osborne and F. Verstraete, Phys. Rev. Lett. **96** (2006) 220503.

[40] G.L. Giorgi, Phys. Rev. A **84** (2011) 054301.

[41] R. Prabhu, A.K. Pati, A.S. De and U. Sen, Phys. Rev. A **86** (2012) 052337.

[42] Sudha, A.R. Usha Devi and A.K. Rajagopal, Phys. Rev. A **85** (2012) 012103.

[43] M. Allegra, P. Giorda and A.Montorsi, Phys. Rev. B **84** (2011) 245133.

[44] X.-J. Ren and H. Fan, Quant. Inf. Comp. Vol. **13** (2013) 0469.

[45] A. Streltsov, G. Adesso, M. Piani and D. Bruss, Phys. Rev. Lett. **109** (2012) 050503.

[46] G.S. Agarwal and K. Tara, Phys. Rev.A 43 (1991) 492.

[47] A. Zavatta, S. Viciani and M. Bellini, Science **306** (2004) 660.

[48] T. Yu and J.H. Eberly, Quant. Inf. Comput. **7** (2007) 459.

[49] W. Dür, G. Vidal, and J. I. Cirac, Phys. Rev. A **62** (2000) 062314.